Chinese Chemical Letters 31 (2020) 2799–2802

Contents lists available at ScienceDirect

Chinese Chemical Letters

journal homepage: www.elsevier.com/locate/cclet

Communication

Field measurement of the organic peroxy radicals by the low-pressure reactor plus laser-induced fluorescence spectroscopy

Shule Li, Keding Lu*, Xuefei Ma, Xinping Yang, Shiyi Chen, Yuanhang Zhang

State Key Joint Laboratory of Environmental Simulation and Pollution Control, College of Environmental Sciences and Engineering, Peking University, Beijing 100871, China

ARTICLE INFO

Article history:
Received 15 June 2020
Received in revised form 7 July 2020
Accepted 29 July 2020
Available online 31 July 2020

Keywords:
Organic peroxy radicals
Flow tube reactor
LIF
RO_2 measurement
Field observation
Ozone production rate

ABSTRACT

A low-pressure reactor (LPR) was developed for the measurement of ambient organic peroxy (RO_2) radicals with the use of the laser-induced fluorescence (LIF) instrument. The reactor converts all the RO_x (= RO_2 + HO_2 + RO + OH) radicals into HO_2 radicals. It can conduct different measurement modes through altering the reagent gases, achieving the speciated measurement of RO_2 and $RO_2^{\#}$ (RO_2 radicals derived from the long-chain alkane, alkene and aromatic hydrocarbon). An example of field measurement results was given, with a maximum concentration of 1.88×10^8 molecule/cm^3 for RO_2 and 1.18×10^8 molecule/cm^3 for $RO_2^{\#}$. Also, this instrument quantifies the local ozone production rates directly, which can help to deduce the regional ozone control strategy from an experimental perspective. The new device can serve as a potent tool for both the exploration of frontier chemistry and the diagnosis of the control strategies.

Ambient organic peroxy (RO_2) radical is almost the only highly reactive intermediate produced during the oxidation processes of hydrocarbons [1,2]. As a prominent media, RO_2 radical is closely related to the removal of primary pollutants and the generation of secondary pollutants. Together with hydroperoxy (HO_2) and hydroxyl (OH) radicals, RO_2 radicals determine the atmospheric oxidation capacity, and therefore significantly influence the formation of secondary pollutants, including tropospheric ozone (O_3), organic nitrates, organic acids, and particulate matters [3–7].

The atmospheric abundance and distribution of RO_2 radicals are crucial for a better understanding of tropospheric chemical oxidation [8]. The quantitative detection of RO_2 is not only a critical data foundation but a useful parameter in the chemical model as well [8,9]. However, since RO_2 is highly reactive with trace gases and surfaces, similar to the other free radicals, a sensitive and precise detection system is required to measure ambient RO_2, which is technically challenging to achieve.

The first field measurement approach of RO_2 radicals was put forward in 1978 [10], known as the matric isolation and electron spin resonance (MIESR). It is a direct measurement technique and can distinguish different RO_2 species. However, complex operation and harsh sample storage conditions limit the application of this technique [10–12]. The peroxy radical chemical amplifier (PERCA), first proposed in 1984 [13], is one of the most widely used methods due to its high operability, but it can hardly separate different RO_2 species [13–17]. The same problem happens to the peroxy radical chemical ionization mass spectrometry (PerCIMS (or RO_xMAS) technique, although it has higher accuracy and shorter chain length requirement [9]. The laser-induced fluorescence (LIF) is a classic technique of measuring OH and HO_2 [18,19]. Some progress has been made in measuring RO_2 radicals by combining LIF with a chemical flow tube reactor [20], but only a few field observations of RO_2 radicals have been reported before [21,22].

In this work, a flow tube reactor was developed based on the previous works [20,23] and was applied together with the Peking University LIF instrument, implementing the measurement of ambient RO_2 radicals. By utilizing the active chemical priorities of some types of RO_2 (long-chain alkane-, alkene- and aromatic hydrocarbon-derived) radicals (known as $RO_2^{\#}$) [21], speciated detection of these types of RO_2 was achieved.

The measurement of ambient RO_2 by LIF technique involves two steps of chemical conversion: a) RO_x (= RO_2 + HO_2 + RO + OH) radicals are converted into HO_2 radicals inside the flow tube reactor under a low-pressure condition; b) HO_2 radicals obtained at the exit of the flow tube are further converted into OH radicals in the fluorescence cell, where OH can be detected directly, under an even lower pressure condition. These processes are illustrated in Fig. 1.

Inside the flow tube reactor, nitric oxide (NO) and carbon monoxide (CO) are introduced as reagent gases. With excessive NO, RO_2 can quickly convert to organic oxy radicals (RO), followed

* Corresponding author.
E-mail address: k.lu@pku.edu.cn (K. Lu).

https://doi.org/10.1016/j.cclet.2020.07.051
1001-8417/

by the formation of HO_2 and carbonyl compounds (R'O) with the presence of oxygen (O_2) in sampled air (Reactions 1 and 2). Generated HO_2, as well as the initially existed HO_2 in sampled air, can further react with NO, resulting in the generation of OH radicals (Reaction 3):

$$RO_2 + NO \rightarrow RO + NO_2 \quad (1)$$

$$RO + O_2 \rightarrow R'O + HO_2 \quad (2)$$

$$HO_2 + NO \rightarrow OH + NO_2 \quad (3)$$

As the chemical reactivity of OH is much higher than that of HO_2, the prolonged residence of OH radical in the flow tube may cause significant radical loss. Excessive CO is simultaneously injected into the reactor, thereby the chemical equilibrium between OH and HO_2 can be shifted to the HO_2 side (Reactions 4 and 5), minimizing the radical loss in the flow tube:

$$CO + OH \rightarrow CO_2 + H \quad (4)$$

$$H + O_2 + M \rightarrow HO_2 + M \quad (5)$$

Nevertheless, the conversion efficiency of RO_2 to HO_2 is still inevitably limited due to several radical loss processes. Firstly, all the RO_x radicals can undergo termolecular recombination reactions with NO (Reactions 6-9):

$$RO_2 + NO + M \rightarrow RONO_2 + M \quad (6)$$

$$RO + NO + M \rightarrow RONO + M \quad (7)$$

$$HO_2 + NO + M \rightarrow HONO_2 + M \quad (8)$$

$$OH + NO + M \rightarrow HONO + M \quad (9)$$

Secondly, reactive collisions of RO_x radicals with the inner surface of the reactor are also major loss processes need to be considered (Reactions 10–13):

$$RO_2 + wall \rightarrow products \quad (10)$$

$$RO + wall \rightarrow products \quad (11)$$

$$HO_2 + wall \rightarrow products \quad (12)$$

$$OH + wall \rightarrow products \quad (13)$$

Reactions with NO (Reactions 6–9) are pressure-dependent [20], so they can be suppressed effectively by lowering the pressure in the reactor. Based on the rate constants recommended by previous studies (Table S1 in Supporting information), recombination reactions become insignificant under the low-pressure condition. But wall reactions are still dominant with a reduction of total HO_2 yield of ~20% [20], even after coating the inner surface of the reactor with the Teflon layer.

The central part of the airflow is collected into the fluorescence cell at the exit of the reactor. Additional NO is injected into this unit to shift the chemical equilibrium between HO_2 and OH back to the OH side, which can be detected by the LIF directly. A detailed description of the detection principle can be found in previous papers [18,19]. In brief, OH radicals can be excited by narrow-bandwidth UV laser (λ =308 nm) on a single rovibronic transition, and therefore fluoresce. Gated photon counting is used to produce a time delay to discriminate the emitted fluorescence by OH and laser stray light. The background signal is determined by turning the laser resonance on and off periodically. The conversion between fluorescence signals and radical concentrations requires a calibration.

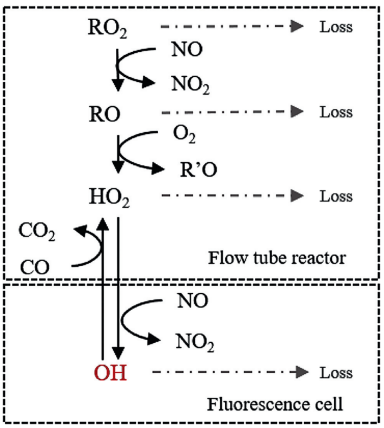

Fig. 1. Chemical reactions in the reactor and fluorescence cell. "Loss" in grey includes the process of wall collision and intermolecular recombination reaction; OH in red is the signal detected by the LIF directly.

When NO and CO are added as reagent gases into the reactor, all the RO_x radicals are converted and detected in the fluorescence cell, so this measurement mode is called "RO_x mode". When only CO is added, RO_2 and RO cannot be converted into HO_2 theoretically, so this mode was called "HO_x mode" in previous studies [20]. However, it has been found afterward that for longer chain (C > 3) alkane-, alkene- and aromatic hydrocarbon-derived RO_2 radicals ($RO_2^{\#}$), they can rapidly convert to HO_2 and then OH in the fluorescence cell when the concentration of NO reaches a certain level in the fluorescence cell [23,24]. This characteristic may elevate the signal of HO_2 radicals as an "RO_2 interference", yet it is also a potentiality to measure different RO_2 species by rising NO concentration in the fluorescence cell. In consequence, when only CO is introduced, $RO_2^{\#}$, RO, OH, and HO_2 are measured (named as "$RO_2^{\#}$ mode"). Because the concentration of RO is negligible compared to that of RO_2 and HO_2, so RO_2 and $RO_2^{\#}$ radical concentrations can then be calculated by simultaneously measured OH and HO_2 data.

Based on the measurement principle mentioned above, the flow tube reactor was designed, as can be seen in Fig. 2. The ambient air was sampled into the reactor through a 1 mm orifice (nickel, 70°, Beam Dynamics, Inc.) with a flow rate of 7 slm (standard liters per minute at 1 atm, 20 °C). Reagent gases, NO and CO, were immediately injected into the sampled air through a glass tube (l = 100 mm, i.d. = 4 mm) after the inlet nozzle, attaining ultimate mixing ratios of 0.7 ppmv and 0.17% respectively. These concentrations were defined based on the simulation results of MCM 3.2 ([20]). The flow tube (l = 830 mm, i.d. = 66 mm) is made of quartz, and its inner surface is coated with the Teflon layer. The reactor was operated at ~25 hPa. The pressure was controlled by a butterfly valve and monitored by a vacuum gauge (Edwards, APG100). Excess air in the reactor was removed by an oil-free vacuum pump (Edwards, XDS35i).

At the end of the flow tube, another nozzle (4 mm orifice, stainless steel, 70°) was used to sample the central part of the

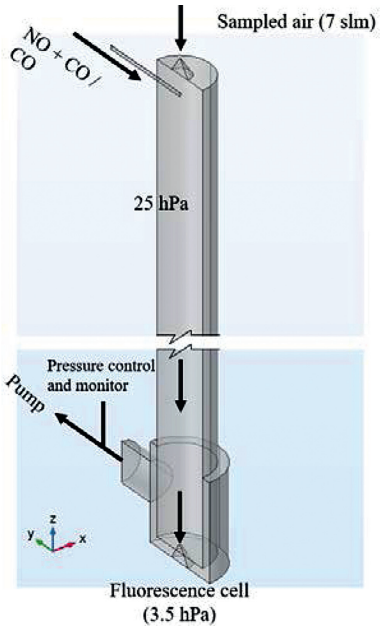

Fig. 2. Schematic diagram of the flow tube reactor (partially broken).

reacted gas to the fluorescence cell, in which the pressure was kept at ~4 hPa. Pure NO (Linde AG, 99.5%) was used to convert HO_2 to OH, so that both RO_2 and $RO_2^{\#}$ can be detected in this work.

All the reagent gases were controlled by mass flow controllers (HORIBA METRON, S48 300/HMT). Electromagnetic valves and time relays were used to achieve periodically (5 min) switch between the two measurement modes. Thus, continuous online measurement with alternating modes has a time resolution of 10 min for both RO_2 and $RO_2^{\#}$.

Based on previous studies, equal concentrations of OH and HO_2 can be generated by the photolysis (λ =185 nm) of H_2O at 1 atm [19,25]. It has also been proven that equal amounts of HO_2 and RO_2 can be produced when the suitable hydrocarbon is mixed with humid air [8,20,26], as long as the introduced hydrocarbon is stabilized under 185 nm ultraviolet (UV). Hence, it is feasible to calibrate the system by using a radical source designed for OH and HO_2 calibration (for a detailed description of the calibration source, see reference [20]).

The calibration method depends on the approaches to obtaining OH and HO_2 data. If all the RO_2, HO_2, and OH are measured simultaneously by one LIF instrument, the detection sensitivities can be determined in three steps by altering reagent gases in the calibration source: a) Humid air with CO; b) humid air with hydrocarbon; c) only humid air. The fluorescence photon count rate (counts/s) of each radical species can then be calculated directly. The calculation method can be found in the previous paper [20].

However, if the OH and HO_2 data are obtained from another instrument, which is the case of this work, the photon count rate cannot be calculated directly. Concentrations of RO_x, HO_2, and OH need to be calculated before doing the subtraction. In this case, three parameters should be considered: a) Conversion efficiency of RO_2 to HO_2 in the reactor (r_1), b) conversion efficiency of HO_2 to OH in the fluorescence cell (r_2), c) the sensitivity of HO_2 radicals (S_{HO_2}/$[HO_2]_0$).

Since pure NO is used in the fluorescence cell, 100% HO_2 is assumed to be converted into OH ($r_2 = 1$). The conversion efficiency of RO_2 to HO_2 is referenced by CH_3O_2, which was simulated by the Master Chemical Mechanism (MCM v3.3). The sensitivity of RO_x radicals can be calculated *via* Eq. 1:

$$C_{RO_x} = \frac{S_{HO_2}}{[HO_2]_0 \times r_1} \quad (1)$$

An ambient air measurement was performed in summer 2019, at a wetland park in Chengdu, China (30.4259°N, 103.847126°E). The site is in the suburbs, surrounded by plenty of vegetation. However, because of the nearby China Civil Aviation Flight Academy, many helicopters were flying above the site during the campaign, which may lead to primary emissions of pollutants. The instrument was placed ~10 m above ground, adjacent to the other LIF (used to measure HO_2 and OH).

Fig. 3 shows the averaged diurnal profiles of RO_2 and $RO_2^{\#}$ radicals from 26th August to 12th September. The variations of RO_2 and $RO_2^{\#}$ were highly correlated with HO_2 radicals. These photochemically formed radicals peaked at around 14:00 with concentrations of 1.55×10^8 (RO_2), 1.04×10^8 ($RO_2^{\#}$), and 1.50×10^8 (HO_2) molecule/cm^3, when the solar actinic flux reached the highest value. In the meanwhile, NO concentration reached the lowest values at noon and peaked in the early morning with a concentration of ~8 ppbv. An apparent negative correlation between peroxy radicals and NO can be observed. A small peak of RO_2 and $RO_2^{\#}$ radicals was found at around 20:00, indicating the existence of radical source in the evening. A strong positive correlation between NO_3 and RO_2 radicals has been found in a previous study [27], implying the rising NO_3 radicals may be the possible reason for this small peak at night. The concentration level and diurnal pattern of RO_2 are similar to what has been reported in previous studies [20–23], besides the $RO_2^{\#}/RO_2$ (~60% in this case) was a little higher than before. The divergence between $RO_2^{\#}$ and RO_2 can hardly be observed in the early morning when NO concentration was increasing rapidly. A possible reason is that the ambient NO promoted the conversion of RO_2 in the converter or even in the atmospheric, invalidating the separation of $RO_2^{\#}$ radicals. Volatile organic compounds (VOCs) were also measured in this campaign (Table S2 and Fig. S1 in Supporting information). Ethene was the most abundant VOC with a proportion of 4.49% that can generate $RO_2^{\#}$, while ethyne was the most abundant among all the VOCs. The ratio of $RO_2^{\#}$-produced VOCs to total VOCs was about 35.5%.

The photochemical O_3 production rate ($P(O_3)$) can be calculated by the oxidation rate of NO to NO_2 through its reaction with peroxy radicals (HO_2 and RO_2, Reactions 1–3) [28–30]. Without considering the loss processes of NO_2 (*e.g.*, the reaction of NO_2 and OH or the

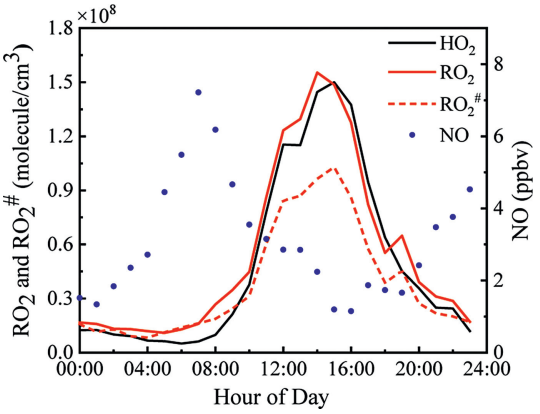

Fig. 3. The diurnal means of RO2, RO2#, HO2, and NO (1 -h average).

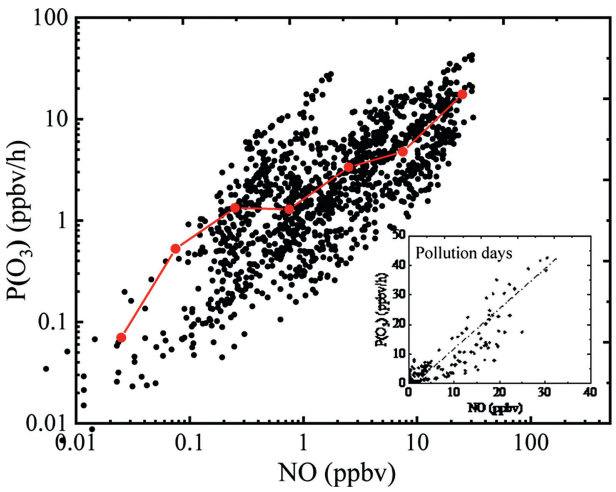

Fig. 4. NO dependence of $P(O_3)$ and the correlation between NO and $P(O_3)$ in pollution days.

formation of organic nitrates by RO_2), the upper limit for $P(O_3)$ can be estimated by Eq. 2 [31],

$$P(O_3) = [NO][HO_2]k_{NO+HO_2} + [NO][RO_2]k_{NO+RO_2} \quad (2)$$

where k_{RO_2}+NO and k_{HO_2}+NO denote the rate constants of the reaction of RO_2 + NO and HO_2 + NO. Fig. 4 shows the dependence of $P(O_3)$ on NO. The $P(O_3)$ increased with the rising of NO concentration, except for a small decline of around 1 ppbv of NO. The correlation between NO and $P(O_3)$ in pollution days has also been reported in Fig. 4 with a relatively strong positive correlation ($R^2 = 0.78$), indicating that the suburb Chengdu is NO_x sensitive for the ozone production.

In conclusion, a low-pressure flow tube reactor coupling with the LIF instrument was developed and successfully applied in the field measurement of RO_2 and $RO_2^{\#}$. RO_2 radicals were firstly converted to HO_2 radicals in the reactor and then to OH in the fluorescence cell. Longer chain (C > 3) alkane, alkene and aromatic hydrocarbon-derived RO_2 radicals ($RO_2^{\#}$) can be determined separately due to their selective chemical properties. The results of field measurements have proven that the designed reactor is an effective and convenient extension for the LIF technique. High NO concentration may affect the speciated measurement results, which limits the application of this technique in urban areas. Further studies on improving the performance of speciated measurements are still needed.

Declaration of competing interest

The authors declare that they have no known competing financial interests or personal relationships that could have appeared to influence the work reported in this paper.

Acknowledgments

The work was supported by the National Key R&D Program of China (No. 2017YFC0209402) and the Beijing Natural Science Foundation, China (No. JQ19031). The authors gratefully acknowledge the support and assistance from Prof. Limin Zeng and Prof. Xin Li in the field campaign of Chengdu.

Appendix A. Supplementary data

Supplementary material related to this article can be found, in the online version, at doi:https://doi.org/10.1016/j.cclet.2020.07.051.

References

[1] G.P. Brasseur, J.J. Orlando, G.S. Tyndall, Atmospheric Chemistry and Global Change, Oxford University Press, New York, 1999.
[2] T. Berndt, W. Scholz, B. Mentler, et al., Angew. Chem. Int. Ed. 57 (2018) 3820–3824.
[3] Q. Zou, H. Song, M. Tang, K. Lu, Chin. Chem. Lett. 30 (2019) 2236–2240.
[4] R. Atkinson, D.L. Baulch, R.A. Cox, et al., J. Phys. Chem. Ref. Data 26 (1997) 521–1011.
[5] R. Atkinson, J. Arey, Chem. Rev. 103 (2003) 4605–4638.
[6] R. Atkinson, J. Arey, S.M. Aschmann, Atmos. Environ. 42 (2008) 5859–5871.
[7] X.P. Yang, H.C. Wang, Z.F. Tan, K.D. Lu, Y.H. Zhang, Acta Chim. Sin. 77 (2019) 613–624.
[8] M. Hanke, J. Uecker, T. Reiner, F. Arnold, Int. J. Mass Spectrom. 213 (2002) 91–99.
[9] T. Reiner, M. Hanke, F. Arnold, J. Geophys. Res. 102 (1997) 1311–1326.
[10] D. Mihelcic, D.H. Ehhalt, G.F. Kulessa, et al., Pure Appl. Geophys. 116 (1978) 530–536.
[11] D. Mihelcic, P. Musgen, P. Müsgen, D.H. Ehhalt, J. Atmos. Chem. 3 (1985) 341–361.
[12] D. Mihelcic, A. Voltz-Thomas, A. Volz-Thomas, et al., J. Atmos. Chem. 11 (1990) 271–297.
[13] C.A. Cantrell, D.H. Stedman, Geophys. Res. Lett. 9 (1982) 846–849.
[14] D.R. Hastie, M. Weissenmayer, J.P. Burrows, G.W. Harris, Anal. Chem. 63 (1991) 2048–2057.
[15] J. Hu, D.H. Stedman, Anal. Chem. 66 (1994) 3384–3393.
[16] K.C. Clemitshaw, L.J. Carpenter, S.A. Penkett, M.E. Jenkin, J. Geophys. Res. 102 (1997) 25405–25416.
[17] Y. Chen, C. Yang, W. Zhao, et al., Analyst 141 (2016) 587–5878.
[18] F. Holland, M. Hessling, A. Hofzumahaus, J. Atmos. Sci. 52 (1995) 3393–3401.
[19] F. Holland, J. Geophys. Res. 108 (2003) 8246.
[20] H. Fuchs, F. Holland, A. Hofzumahaus, Rev. Sci. Instrum. 79 (2008) 84104.
[21] Z. Tan, H. Fuchs, K. Lu, et al., Atmos. Chem. Phys. 17 (2017) 663–690.
[22] Z. Tan, F. Rohrer, K. Lu, et al., Atmos. Chem. Phys. 18 (2018) 12391–12411.
[23] L.K. Whalley, M.A. Blitz, M. Desservettaz, P.W. Seakins, D.E. Heard, Atmos. Meas. Tech. 6 (2013) 3425–3440.
[24] H. Fuchs, B. Bohn, A. Hofzumahaus, et al., Atmos. Meas. Tech. 4 (2011) 1209–1225.
[25] A. Hofzumahaus, U. Aschmutat, U. Brandenburger, et al., J. Atmos. Chem. 31 (1998) 227–246.
[26] D.J. Creasey, P.A. Halford-Maw, D.E. Heard, M.J. Pilling, B.J. Whitaker, Faraday Trans. 93 (1997) 2907–2913.
[27] A. Geyer, K. Bächmann, A. Hofzumahaus, et al., J. Geophys. Res. 108 (2003) 8249.
[28] A. Volz, D. Mihelcic, P. Müsgen, et al., Tropospheric Ozone: Regional and Global Scale Interactions, Springer, Netherlands, Dordrecht, 1988.
[29] B.A. Ridley, J. Geophys. Res. 97 (1992) 10–388.
[30] L. Kleinman, Y.N. Lee, S.R. Springston, et al., J. Geophys. Res. 100 (1995) 7263–7273.
[31] D. Mihelcic, F. Holland, A. Hofzumahaus, et al., J. Geophys. Res. 108 (2003) 8254.